Subsurface Sensing Technologies and Applications Vol. 4, No. 4, October 2003 (©2003)

Suppressing GPR Clutter from Randomly Rough Ground Surfaces to Enhance Nonmetallic Mine Detection

Carey Rappaport,* Magda El-Shenawee, and He Zhan

Northeastern University, 235 Forsyth Building, Boston, MA 02115

Received January 17, 2000; revised May 22, 2003

This study attempts to quantify the ground penetrating radar rough ground surface clutter by numerical modeling of wave scattering, and establish a strategy to suppress the clutter for given test signals. The goal is to improve the GPR detection statistics for small, buried, low-contrast nonmetallic antipersonnel mines. Using a model of an experimentally measured impulse GPR signal, we simulate the ground surface and buried low-contrast mine target scattered responses. We employ a 2D finite difference time domain (FDTD) method to analyze the pulse shape, delay, and amplitude characteristics of the scattered waves—with and without buried nonmetallic mine targets—as a function of roughness parameters. Five hundred Monte Carlo simulations of various test cases of specified ground root mean square height and correlation length were run to generate statistics for the clutter and target signal variations. In addition, the effectiveness of identifying and removing the ground surface clutter signal for detecting subsurface targets is presented. Results indicate that even with moderate roughness, statistics can be generated to enhance the detection of small, shallow, low-contrast targets.

Key Words. GPR, rough surface, mine detection, clutter suppression.

1. Introduction

The problem of detecting buried dielectric targets—such as nonmetallic antipersonnel mines—with ground penetrating radar (GPR) is important and challenging. Because the dielectric constant and electrical conductivity of the mine target is similar to that of the surrounding soil and its size is comparable to the thickness of soil above it, detection and discrimination are difficult. In addition, the soil dielectric constant may not be well

*To whom all correspondence should be addressed. Phone: (617) 373-2043; fax: (617) 373-8627; e-mail: rappaport@neu.edu

1566-0184/03/1000-0311/0

characterized, and the ground surface will usually be rough, often with surface height variations of the order of the target burial depth. While there are many sources of clutter obscuring the mine target signal—including volumetric inhomogeneities (rocks, roots, metal fragments) and surface vegetation—the largest single source of undesirable signal is the ground surface itself. Since the ground has an infinite surface and presents a larger impedance mismatch with the air above it than with the low-contrast, nonmetallic target within it, its contribution to clutter is quite significant. Further, buried clutter objects can only be inferred by imaging and reconstruction, while the ground surface is unobscured, and its effects can be measured directly.

Impulse ground penetrating radar has been used as a robust and relatively inexpensive means of detecting underground objects [1]. By observing the arrival time of a subsurface scattered pulse and eliminating the reflection from the ground surface by time gating, it is possible to detect deeply buried anomalies. However, when the target is small, shallow, and of low-contrast, special modeling and processing are required to characterize and separate the ground surface clutter from the target signal. A commonly used procedure of background averaging to remove the ground clutter signal can be effective for very smooth ground surfaces, but tends to rapidly degrade for moderate roughness. In this study, we simulate the effects of rough ground on the GPR signal using Monte Carlo FDTD modeling of random surface variation. Because of the need for multiple case studies of hundreds of Monte Carlo runs, we used a very fast 2-D TM FDTD code, specifically adapted to frequency dependent, lossy media, with a lossy Perfectly Matched Layer (PML) absorbing boundary condition [2–4]. Clearly, more accurate modeling is afforded with a three-dimensional FDTD model, but each set of 500 runs would require 2000 hours of supercomputer CPU time. Instead, this study presents a range of possible signal delay, attenuation, and distortion characteristics, with associated statistical variation as a function of ground surface roughness.

As a baseline, we model the wave scattering for a bistatic impulse GPR geometry, based on the Geo-Centers, Inc. EFGPR mine detection system, as shown in Figure 1. The nonmetallic mine-like target is modeled as a rectangle of TNT with frequency independent $\varepsilon = 2.9\,\varepsilon_0$ and $\sigma = 0.0001$ S/m [5]. The thin plastic mine casing is not included in the model, as it has almost the same dielectric constant as TNT in the given frequency range, and contributes insignificantly to target scattering. The modeled excitation pulse, presented as a function of time in Figure 2, is based on the signal measured using the Geo-Centers TEMR antenna elements as transmitters and receivers [6]. It is wideband, with frequency response (6 dB roll-off) from 700 MHz to 1.3 GHz. This frequency range is ideal for detecting antitank mines, which are thicker and more deeply buried than antipersonnel mines. Although this frequency range is a little too low for optimal discrimination of objects with

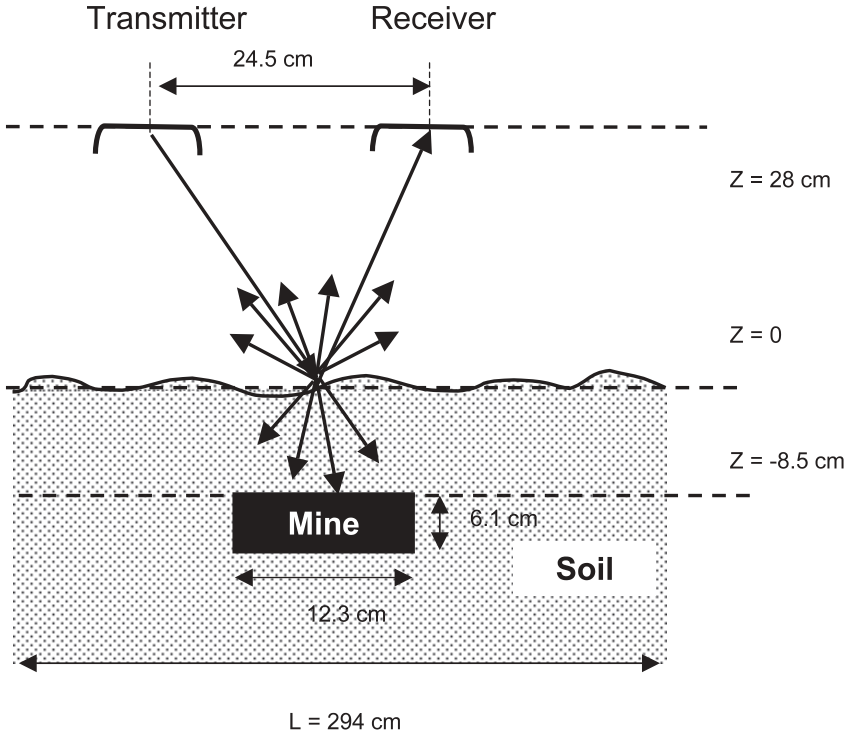

Figure 1. Bistatic ground penetrating radar scattering configuration with rough ground surface and buried mine target, based on the Geo-Centers, Inc. EFGPR system.

scale lengths of the order of 5 cm, it is experimentally realizable. The TEMR element radiates a fairly broad beamwidth nearfield antenna pattern, with wideband half-power points at roughly $\pm 60^{\circ}$ relative to boresight. The FDTD time and space steps used are $\Delta t = 20$ ps and $\Delta = 1.22$ cm, maintaining a Courant condition $r = 0.5$. Simulations are run for 500 surface realizations—with and without a mine target at a typical burial depth of 8.5 cm below the nominal surface level—for a variety of roughness statistics.

2. Rough Surface Model Formulation

Assuming that the random height of the ground surface has a Gaussian distribution with zero mean and standard deviation equal to σ_h, the probability density function of the height z is [7]:

$$p(z) = \frac{1}{\sigma_h \sqrt{2\pi}} \exp(-z^2/2\sigma_h^2) \tag{1}$$

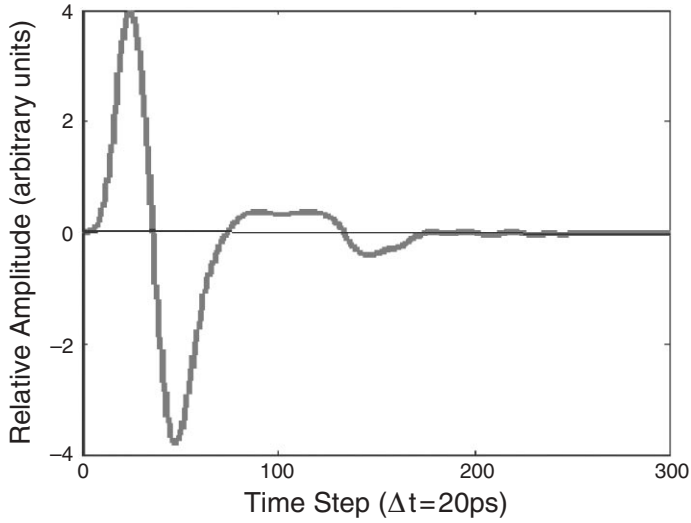

Figure 2. Measured time pulse transmitted by the Geo-Centers, Inc. EFGPR antenna element. Time units are in 20 ps time steps, amplitude is given in arbitrary relative intensity units.

This statistical distribution of the height provides no information about the distances between the hills and the valleys of the surface [7]. An additional function is needed to describe the density of the surface irregularities of the rough surface. This function is the autocorrelation function or its Fourier Transform, the surface profile power spectral density function. The auto-correlation function $R(x_d)$ gives the correlation between the random heights at two different points on the surface, x_1 and x_2. It is defined by [7,8]:

$$R(x_d) = \frac{\langle f(x_1) f(x_1 + x_d) \rangle}{\sigma_h^2} \tag{2}$$

where $x_d = x_2 - x_1$, and the brackets denote averaging over the arguments. For full correlation, $\lim_{x_d \to 0} R(x_d) = 1$, and for independence, $\lim_{x_d \to \infty} R(x_d) = 0$. Moreover, if the surface profile spectral density function $W(k_x)$ is given, then the auto-correlation function $R(x_d)$ can be obtained by the inverse Fourier Transform as:

$$R(x_d) = \frac{1}{\sigma_h^2} \int_{-\infty}^{\infty} W(k_x) \exp(ik_x x_d)\, dk_x \tag{3}$$

If the surface spectral density $W(k_x)$ is assumed to be Gaussian as [8,9]

$$W(k_x) = \frac{l_c s_h^2}{2\sqrt{p}} \exp\left(\frac{-k_x^2 l_c^2}{4}\right) \tag{4}$$

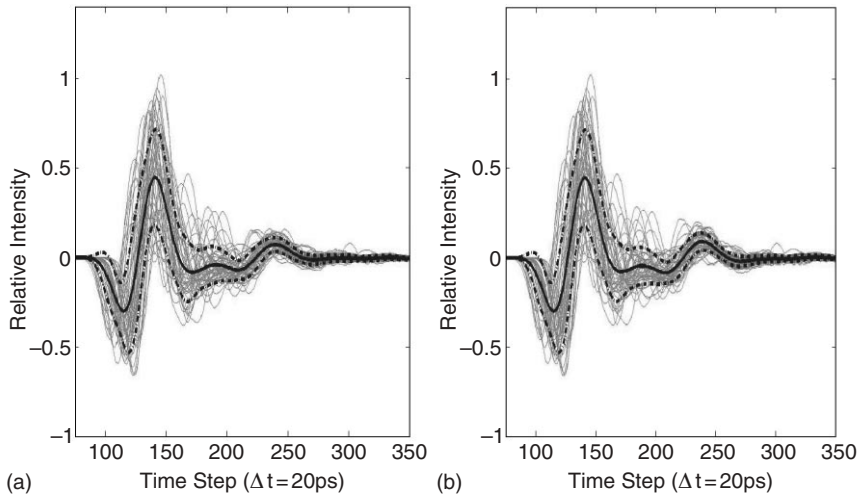

Figure 3. One hundred sample Monte Carlo dispersive FDTD calculations of field intensity as a function of time, received after scattering from a half space of Puerto Rican clay loam (10% moisture and 1.4 g/cc density) with randomly rough ground surface (Gaussian parameters: $\sigma_h = 3$ cm and $l_c = 10$ cm) for: a) soil alone, and b) soil with a 12.3 cm by 6.1 cm rectangular region of TNT buried 8.5 cm below the nominal surface. Also shown are the mean signals and curves one standard deviation above and below the means. Note that the differences between the mean signals are too small to distinguish.

in which k_x is the surface profile wave number. Thus from (3), the autocorrelation function will also be Gaussian given by

$$R(x_d) = \exp\left(-\frac{x_d^2}{l_c^2}\right) \tag{5}$$

where l_c is the correlation distance for which $R(x_d)$ will drop to the value e^{-1}.

While other statistical variations for randomly rough ground surfaces may be more applicable for some rough ground surfaces, the Gaussian provides a sufficiently rich family of surface realizations to establish a population for analyzing clutter effects.

Although statistical analysis can be done on the received signals themselves, it is more useful to consider the particular effects on these signals caused by scattering by the rough ground. For example, Figure 3 shows the computed received signals from 100 rough surface realizations of a ground surface with height and correlation length $\sigma_h = 3$ cm and $l_c = 10$ cm, without (Fig. 3a) and with (Fig. 3b) a buried target. The mean signal and confidence level one standard deviation above and below the mean signal are overlaid on each plot. It is clear that there is no discernable difference between the

signals for the buried target plot and the target-free plot. For this realistic short pulse GPR signal, interacting with typical randomly rough ground and small low-contrast target, the target signal is too small relative to the ground reflection signal to be observed by simple time gating. Even for the relative deep 8.5 cm burial depth of the mine in this case, the difference between the received signal with and without the mine is less than random variations of the ground surface clutter.

The longer the correlation length l_c, the more likely the received signal will retain its pulse shape in time, experiencing primarily a shifting in time and a change in amplitude corresponding to greater or lesser propagation distances from source to ground to receiver. Smaller l_c implies more surface variation within the illuminating beam footprint. By identifying these features and measuring their statistics separately, much added information about the clutter becomes available. In addition, compensating for the time shift and amplitude scaling allows the shape of each individual received signal to be examined, and used in the determination of whether a buried target is present.

To identify the amplitude scaling A_i of the received pulse S_i for a given trial, we compute the square root of the total energy in the signal divided by the energy in a suitable reference signal. We use the computed received scattered signal from an ideal soil half-space with a flat boundary as the reference S_f by summing over all N time steps:

$$A_i = \frac{\sqrt{\sum_{n=1}^{N} |S_i(n)|^2}}{\sqrt{\sum_{n=1}^{N} |S_f(n)|^2}} \tag{6}$$

Alternatively, the value of the signal peak could be used for this scaling, but it was determined that energy normalization is superior for rougher surfaces that generate greater pulse distortion.

The time shifting is found by cross-correlating each signal under test with the same reference signal, each normalized to the square root of its energy. The cross-correlation function indicates the inter-dependence of the values of two different processes at two different times:

$$C_{fi}(m) = \frac{\sum_{n=1}^{N-|m|} S_f(n) S_i(n+m)}{\sqrt{\sum_{n=1}^{N} |S_f(n)|^2} \sqrt{\sum_{n=1}^{N} |S_i(n)|^2}} \quad \text{for } m \geq 0 \tag{7a}$$

$$C_{fi}(m) = C_{fi}(-m) \quad \text{for } m < 0 \tag{7b}$$

where $i = 1, 2, 3, \ldots M$ is the rough surface realization index, M is the size of Monte Carlo sample. Note that the normalized cross-correlation of the reference signal $S_f(n)$ with itself has a maximum of unity at $m = 0$; that cross-correlation with a shifted copy has a unity maximum at the index

corresponding to the shift; and that cross-correlation of dissimilar signals will have a maximum less than unity. The maximum value of this cross-correlation function is a measure of the pulse shape distortion from that of the ideal flat ground response $S_f(n)$.

3. Numerical Results

Numerical experiments were performed on the well-measured Puerto Rican clay loam with 10% moisture and 1.4 g/cc density [10]. This soil has dielectric constant varying as $6.1 < \varepsilon' < 6.4$ and electrical conductivity $0.033\ \mathrm{S/m} < \sigma < 0.067\ \mathrm{S/m}$ and wavelength varying from $17.0 < \lambda < 9.5$ cm over the 700 MHz to 1.3 GHz bandwidth. The dispersive FDTD model employed uses the Z-transform supplemental equation model for frequency dependent conductivity [2]. With this model, the real dielectric constant is assumed to be constant and the ratio of electric current density and electric field is given by:

$$\sigma(\omega) = \frac{b_0 + b_1 Z^{-1} + b_2 Z^{-2}}{1 + a_1 Z^{-1}},$$

where $Z = e^{i\omega\Delta t}$ for the frequency ω. For the particular type of Puerto Rican clay loam with time step $\Delta t = 20$ ps, the parameters have been found to be [3]: $b_0 = 0.916249$, $b_1 = -1.67662$, $b_2 = 0.761072$, $a_1 = -0.88$, and $\varepsilon'_{\mathrm{Av}} = 4.167$. Note that since the imaginary part of $\sigma(\omega)$ is non-zero, it will contribute to the real part of the dielectric constant, raising it above the $\varepsilon'_{\mathrm{Av}}$ value to the measured frequency dependent values 6.1 to 6.4.

For each pair of Gaussian height and correlation parameters, 500 FDTD runs were performed on different surface realizations. In each case, the scaling and shift were determined using (6) and (7). An example of the distribution of these characteristics for the pair $\sigma_h = 3$ cm and $l_c = 30$ cm, is shown in Figure 4. The average scaling is 0.995 and the average shift is -55 ps. From these histograms, it is apparent that although the ground heights are normally distributed, the amplitudes and time shifts are not.

With the ultimate goal of target detection, it is important to observe the differences in the received signal when a mine is buried under the rough ground surface. For each surface realization, this difference can be clearly seen by simply subtracting the nominal ground-only signal from the signal with the mine present. In this simulated situation, the clutter would be known a priori and numerically removed. In practice, this is not possible, since the clutter signal is not separately available. It is the goal of these Monte Carlo experiments to reasonably estimate the rough surface clutter effects so that they can be suppressed relative to the mine signal, without the *a priori* knowledge of the ground clutter effect for a given trial.

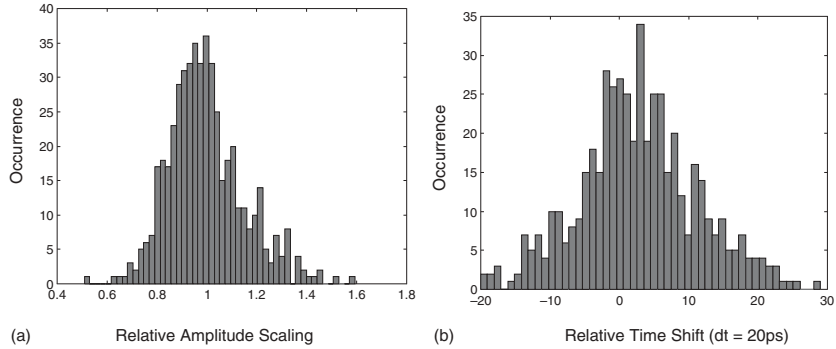

Figure 4. Histograms showing distributions of a) Relative amplitude scaling and b) Relative time shift for received signals scattered by 500 realizations of randomly rough ground (σ_h = 3 cm and l_c = 30 cm).

Using the individual FDTD differences, the responses due to the presence of mines can be compared to the signals from the ground surface alone. The mine position is usually determined by measuring the time delay corresponding to the path to and from the buried target. However, with rough ground, the path from the transmitter to ground to mine and back out to the receiver, changes with the local ground surface height, or the height of the antenna. Since the wave propagation velocity is quite different in air as opposed to soil, the target time delay for a given mine depth varies considerably.

Scatter plots showing the distribution of the shifts of the ground scattered signals $\tau_{\mathrm{gnd}(i)}$ compared to the time delay of the mine scattered signals $\tau_{\mathrm{mine}(i)}$ relative to a nominal perfectly flat ground for different rough surface parameters are shown in Figure 5. For low-contrast targets the dominant aspect of each scattered signal is the ground scattering, so the cross-correlation function gives $\tau_{\mathrm{gnd}(i)}$. To find $\tau_{\mathrm{mine}(i)}$, (7a) is applied to the difference between the signal scattered by the ground and mine and the ground alone (the target signal with *a priori* ground clutter signal removed). The surface root mean square height is σ_h = 3 cm in Figure 5a and 5b while it is 2 cm in Figure 5c and 5d, and 1 cm in Figure 5e and 5f. The correlation length is l_c = 10 cm for the figures on the left and 3 cm for those on the right. There is a strong correlation between $\tau_{\mathrm{gnd}(i)}$ and $\tau_{\mathrm{mine}(i)}$. A regression analysis is conducted to fit these simulated data with a straight line. The slope of this line corresponds to the relative delay between the ground and target scattered signals. The slope is negative, and for very long correlation lengths—corresponding to large, flat raised or lowered portions of ground—would be equal to the $(1-\sqrt{\varepsilon'})$. Since a positive shift in τ_{gnd} indicates the presence of a depression, which in turn implies less soil covering the mine, the time delay for the mine

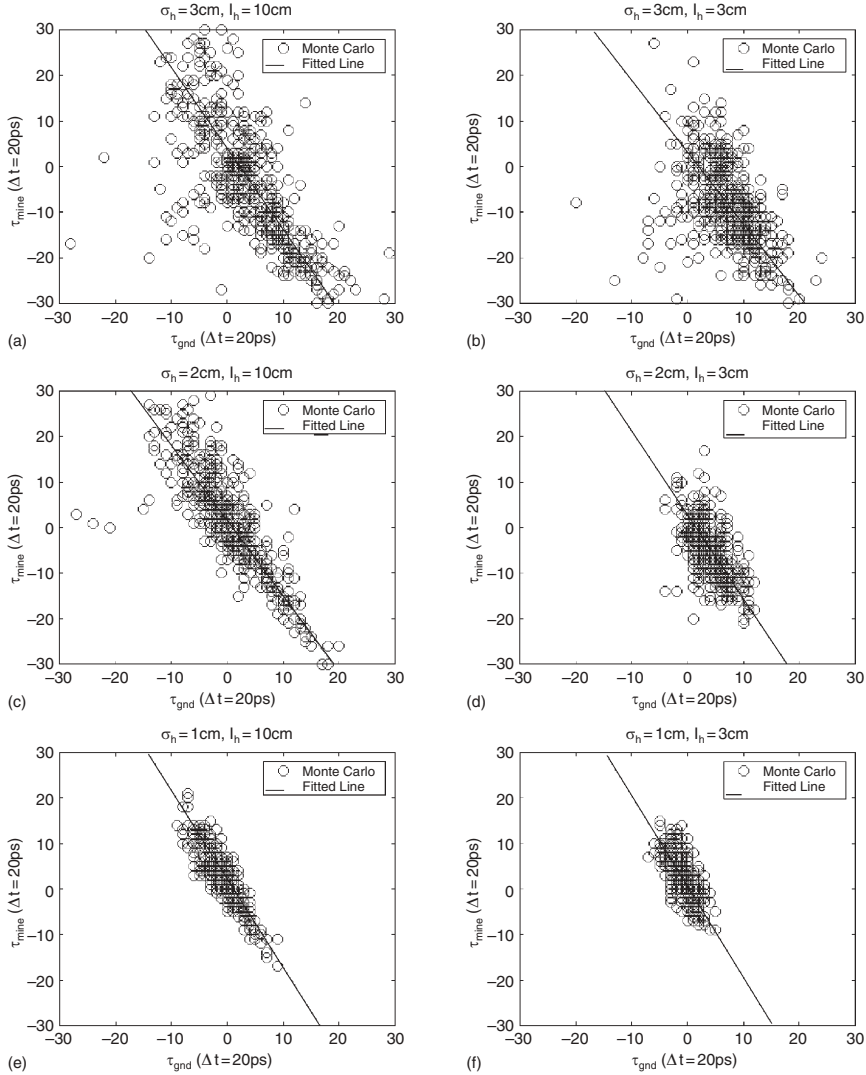

Figure 5. Scatter plots showing the correspondence of time delays of the signal from the mine target buried 8.5 cm below the mean ground height compared to the time shifts due to the ground surface alone for various Gaussian parameters: a) σ_h = 3 cm and l_c = 10 cm, b) σ_h = 3 cm and l_c = 3 cm, c) σ_h = 2 cm and l_c = 10 cm, d) σ_h = 2 cm and l_c = 3 cm, e) σ_h = 1 cm and l_c = 10 cm, f) σ_h = 1 cm and l_c = 3 cm.

signal, τ_{mine}, is reduced by the difference of the wave velocities in air and soil times the depth of the depression. As shown in Figure 5, the fitting error increases with the root mean square slope $\sigma_s = 1.414\,(\sigma_h/l_c)$ [11]. Also, it can be seen that the distribution of points is closer to the mean for small height variation σ_h.

The clutter signal can be suppressed and consequently the target signal can be enhanced using physics-based signal processing. Subtracting the measured or modelled ground surface clutter signal has been a successful strategy to enhance the signal under test [12]. It is possible to improve on this basic algorithm for rougher surfaces using a multiple pass process. First, the average clutter signal is found by shifting each ground-only signal by $-\tau_{\text{gnd}(i)}$, then taking the ensemble average [13]. Note that this is an average over signals, not time, so the resulting signal will be the average pulse shape for the rough ground with delay compensation for the local height variation. Second, this average signal is shifted back by $\tau_{\text{gnd}(i)}$, and scaled by factor A_i in (6) for each mine-in-ground signal and subtracted from these signals. By using the previously modeled (or measured) surface signals to find the ensemble average pulse shape gives the best estimate for the local clutter that corrupts the target signal. Figure 6 shows the result of this subtraction on each of the 100 signals of Figure 3. The differences between the ground-only (Fig. 6a) and mine-present (Fig. 6b) signals are now quite clear, with a peak

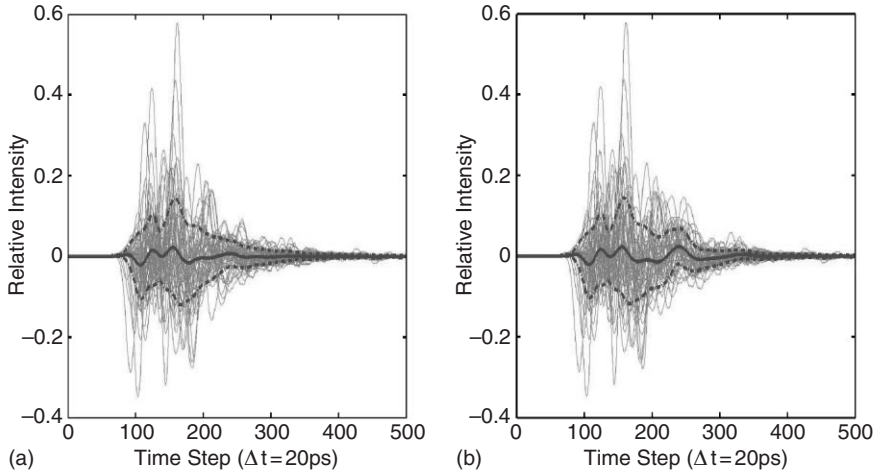

Figure 6. One hundred Monte Carlo calculations of the same physical situation as Figure 3, each processed by subtracting the average ground surface clutter, correlated in time to the sample signal. Note that the amplitude of these processed signals is about one-third of the original signals, and that the mine signal is clearly distinguishable from the mean signal in b) at time step 240, compared to the ground-only mean signal in a).

at about $240\Delta t$. The maximum amplitude of each processed signal is considerably smaller than for each of the original signals in Figure 3, since much of the clutter has been removed. Since the appropriately delayed average ground clutter signal has been subtracted rather than the *a priori* known clutter signal for each trial, the clutter removal is not perfect. The ensemble averages for the ground-only and mine-in-ground cases in Figure 6 indicate that for the particular soil type, mine depth, and radar excitation, the presence of signal at a certain time interval and above a given threshold (average about 0.025) corresponds to a buried target. This provides the basis for a statistical target detection procedure. The results for this example case do not apply for all cases, but the strategy for suppressing ground surface clutter is generally applicable, as long as the mine is not too close to the surface, or the excitation pulse too long. This approach could be used in realistic field measurements, without separately measuring the ground roughness or knowing if a target was present.

If the surface scattered wave was primarily due to a single specular reflection—as would be the case if l_c was large—then this procedure would suppress most of the surface clutter. However, it is possible that the surface scattering occurs at multiple points. In this case, the cross-correlation/shifted ensemble averaging and subtracting procedure is repeated. This process is shown schematically in the flowchart of Figure 7. The initial box labeled "Raw Signals" refers to either the 500 Monte Carlo FDTD

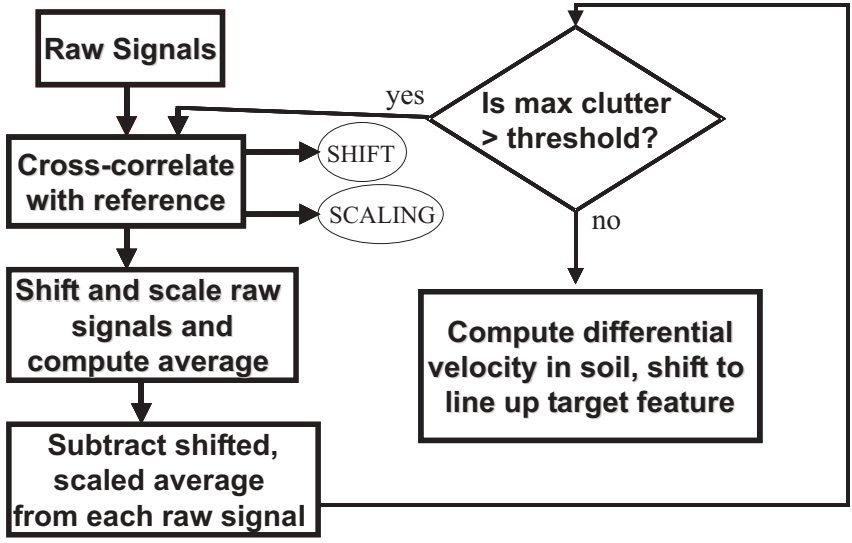

Figure 7. Flowchart of the ground clutter suppression algorithm.

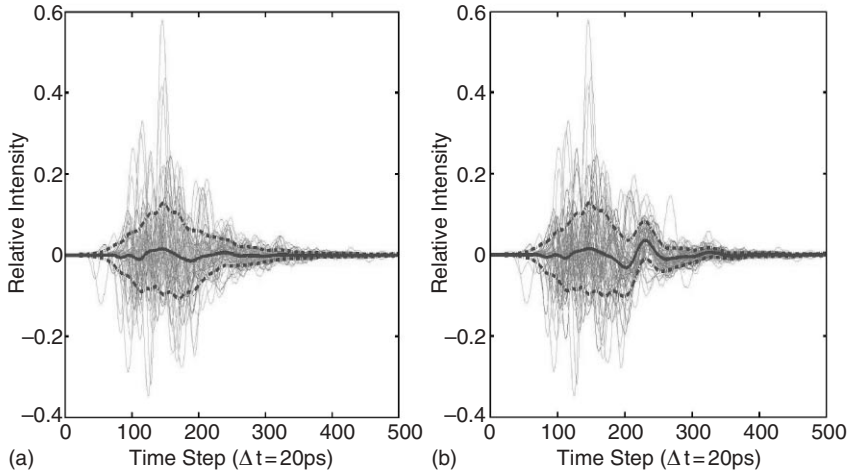

Figure 8. One hundred Monte Carlo calculations of the same physical situation as Figure 3, each processed by multiple subtraction of the average ground surface clutter, correlated in time to the sample signal, as indicated by the flowchart of Figure 7. Almost all the clutter is removed in the mean ground-only signal a), while for the buried mine simulations b), the mine signal is practically the only response. This algorithm is superior if there are sufficient independent views of the ground sample.

simulated signals or actual measured data, obtained progressively with updated averaging.

The signals produced from these multiple subtractions represent the signals scattered just from the target. The obtained shifts τ_i are amplified by the slope values of the straight lines shown in Figure 5 and then used to align these target-only signals. Figure 8 shows the result of multiple subtraction and shifting to realign the mine signals. The average target peak amplitude increases by this realignment to 0.039, or 45% greater—and the average clutter is reduced to 0.019 or 37% lower—than the average levels obtained by just removing ground surface clutter (as shown in Fig. 6). Note that this realignment would have to be performed for every presumed mine depth. This procedure can be performed during actual GPR operation in the field, using several ground-only calibration measurements as the average signal. For hardware focused systems, the ground surface clutter suppression must occur at each receiver, before the signals from multiple receivers are combined.

The average clutter suppressed signals for ground with mine present have been obtained for the same Gaussian roughness parameters of Figure 5, and shown in Figure 9. Also shown are curves indicating one standard deviation above and below the mean. As expected, the standard deviation is

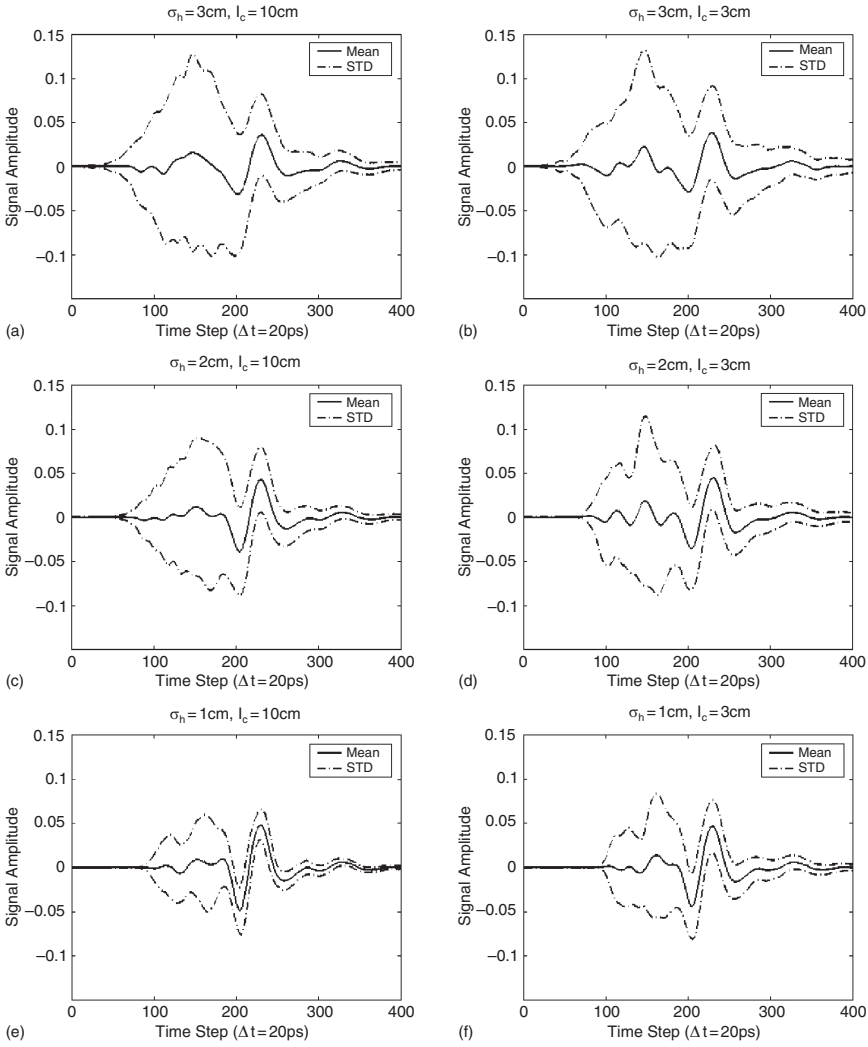

Figure 9. Mean and ±1 standard deviation for 500 Monte Carlo simulations for randomly rough ground with Gaussian parameters a) $\sigma_h = 3$ cm and $l_c = 10$ cm, b) $\sigma_h = 3$ cm and $l_c = 3$ cm, c) $\sigma_h = 2$ cm and $l_c = 10$ cm, d) $\sigma_h = 2$ cm and $l_c = 3$ cm, e) $\sigma_h = 1$ cm and $l_c = 10$ cm, f) $\sigma_h = 1$ cm and $l_c = 3$ cm.

much smaller for the target signal than for the clutter signals. Also visible in Figure 9 is the increase of clutter with the surface mean square slope σ_s. Correlating any trial signal for a given statistical ground roughness and the

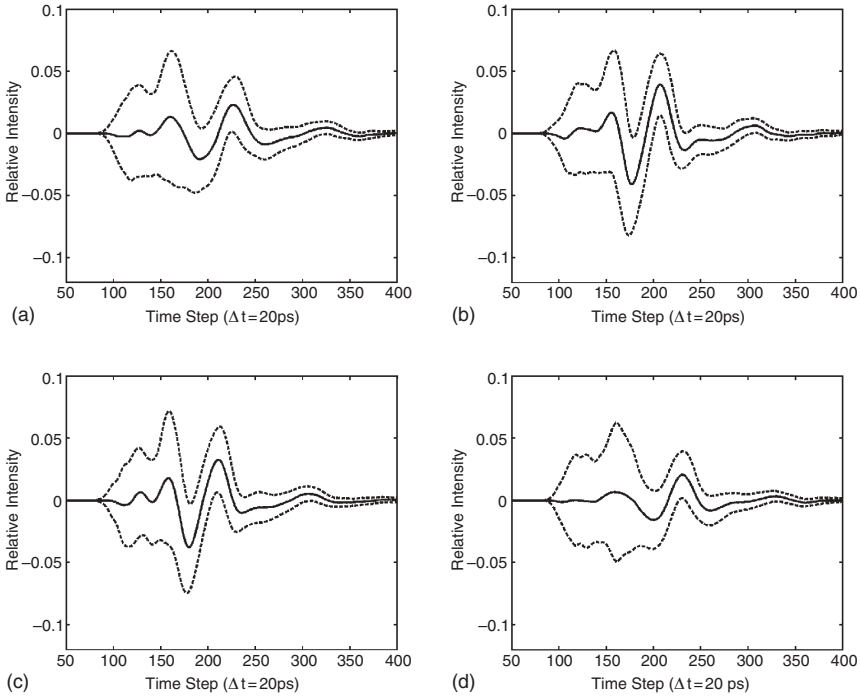

Figure 10. Mean and ±1 standard deviation of 500 Monte Carlo realigned signals for four bistatic geometries, each with ground surface and buried depth parameter settings ($\sigma_h = 1$, $l_c = 10$, $z = 4.8$) cm; center position of transmitter/receiver pair: a) 24.2 cm to the left, b) 12.2 cm to the left, c) 12.2 cm to the right, d) 24.2 cm to the right.

average signal for that roughness with inverse weighting by the standard deviation provides a strong parameter for estimating the presence of a mine at a given position.

Figure 10 shows similar curves as Figure 9, but for a different target depth and for different transverse GPR antenna positions. The four plots represent the averages of 500 clutter suppressed signals for ground having the same roughness statistics with the same two dimensional target buried 4.5 cm below the nominal ground surface, along with the one standard deviation confidence intervals. Each plot shows the signals for the same transmitter/receiver pair spacing, but with a different bistatic GPR geometry relative to the target: with the pair far to the left of the target, just to the left, just to the right, and far to the right. Note that for each plot, the set of curves closely resemble those of Figure 9e, with the strongest amplitude corresponding to the scattered signal from the mine target. The time corresponding to this feature occurs later when the transmitter/receiver pair is farther from the

target, Figures 10a and 10d. When the pair is closer to the target, but not directly over it, Figures 10b and 10c, the mine scattered feature is stronger and occurs at about the same instant as when the target is deeper and the pair is centered above it, Figure 9e. Thus, the clutter suppression algorithm works for various depths and for asymmetric sensing geometries.

Note that in Figures 9 and 10 the ground signal is detected for each trial signal, so that any given ground roughness variations, or even radar antenna height variations are accounted for. That is, if the GPR bounces or sags at a given measurement sample, the ground signal would still be correlated with the shape of the average ground signal, and the appropriate shift is determined.

4. Conclusions

Identifying the time shift and amplitude scaling of the ground surface clutter by correlation with the ideal flat ground provides a means for ground surface clutter removal for a given signal. Shifting this clutter-suppressed signal by a time delay roughly proportional to the differential propagation velocity in the effective soil layer (or absence of soil) relative to the nominal soil level realigns the target signal to its expected temporal position. Using this procedure, even fairly shallow buried nonmetallic mines signals can be distinguished from rough ground surface clutter using available (nonideal) impulse GPR sources.

Although this study is based on two-dimensional synthetic modeling, it presents a representative set of randomly cluttered signals, and shows that the physics-based processing suppresses clutter and leads to enhanced target detection. The problem of mine detection is certainly more complicated than detecting anomalous signals generated by subsurface objects. The issue of distinguishing the particular mine target, as opposed to other buried objects: rocks, roots, pockets of water, is not addressed in this study. However, combining the information from multiple views from different radar positions will help characterize the shape of the anomaly. In addition, fusing information from other modalities—such as electromagnetic induction, acoustic, and infrared detection—with GPR will help reduce false alarms, giving some hope in the effort to characterizing buried mines.

Acknowledgments

This work is supported by the Army Research Office grant No. DAAG55-97-0013 and by CenSSIS, the Center for Subsurface Sensing and Imaging Systems, under the Engineering Research Centers Program of the National Science Foundation, award number EEC-9986821.

References

1. Peters, L. and Young, J., 1986, Applications of subsurface transient radars, I, in Miller, E. (ed.), Time Domain Measurements in Electromagnetics: Van Nostrand Reinhold, New York.
2. Weedon, W. and Rappaport, C., 1997, A general method for FDTD modeling of wave propagation in arbitrary frequency-dispersive media: IEEE Trans. Ant. Prop., v. 45, p. 401–410.
3. Rappaport, C., Wu, S., and Winton, S., 1999, FDTD wave propagation modeling in dispersive soil using a single pole conductivity model: IEEE Trans. Magnetics, v. 35, p. 1542–1545.
4. Rappaport, C. and Winton, S., 2000, Using the PML ABC for air/soil wave interaction modeling in the time and frequency domains: International Journal of Subsurface Sensing Technologies and Applications, v. 1, p. 289–304.
5. von Hippel, A.R., 1953, Dielectric Materials and Applications: Technology Press of M.I.T. and John Wiley, New York.
6. Sahin, A., Rappaport, C., and Dean, A., 1998, Design considerations for short time pulse TEMR antennas using finite difference time domain algorithm: SPIE Aerosense Conf., Orlando, FL, p. 784–793.
7. Beckmann, P. and Spizzichino, A., 1963, The Scattering of Electromagnetic Waves from Rough Surfaces: Macmillan, New York.
8. Thorsos, E., 1988, The validity of the Kirchhoff approximation for rough surface scattering using a Gaussian roughness spectrum: J. Acoust. Soc. Am., v. 83, no. 1, p. 78–92.
9. Mood, A., Graybill, F., and Boes, D., 1974, Introduction to the Theory of Statistics: McGraw-Hill, New York.
10. Hipp, J., 1974, Soil electromagnetic parameters as functions of frequency, soil density, and soil moisture: Proc. of IEEE, v. 62, no. 1, p. 98–103.
11. Bass, F. and Fuks, I., 1979, Wave Scattering from Statistically Rough Surfaces: Pergamon, New York.
12. El-Shenawee, M. and Rappaport, C., 2000, Quantifying the effects of different rough surface statistics for mine detection using the FDTD technique: Proc. SPIE.
13. Warrick, A., Azevedo, S., and Mast, J., 1998, Prediction of buried mine-like target radar signatures using wideband electromagnetic modeling: Proc. of SPIE, v. 3392, p. 776–783.